

Supplementary Material for the manuscript DMD#84194

Hepatic OATP-mediated clearance in the Beagle dog: assessing in vitro-in vivo relationships and applying cross species empirical scaling factors to improve prediction of human clearance

Norikazu Matsunaga, Ayşe Ufuk, Bridget L. Morse, David W. Bedwell, Jingqi Bao, Michael A. Mohutsky, Kathleen M. Hillgren, Stephen D. Hall, J. Brian Houston, and Aleksandra Galetin

Centre for Applied Pharmacokinetic Research, University of Manchester, UK (N.M., A.U., J.B.H., and A.G.), Pharmacokinetic Research Laboratories, Ono Pharmaceutical Co., Ltd., Japan (N.M.), and Lilly Research Laboratories, Eli Lilly and Company, USA (B.L.M., D.W.B., J.B., M.A.M., K.M.H., and S.D.H.)

Table S1: LC-MS/MS conditions for in vitro uptake and K_p experiments

Analyte (<i>m/z</i>)	Internal Standard (<i>m/z</i>)	Mobile Phase
Atorvastatin (559.3 → 440.4)	Diazepam (285.1 → 257.1)	A, B, D
Atorvastatin lactone (541.4 → 448.4)	Diazepam (285.1 → 257.1)	A, B, D
Cerivastatin (460.3 → 356.2)	Diazepam (285.1 → 257.1)	A, B, D
Fexofenadine (502.3 → 466.2)	Flunitrazepam (314.0 → 268.2)	C, D
Pitavastatin (422.3 → 290.3)	Atorvastatin (559.3 → 440.4)	A, B, C, D
Pravastatin (447.3 → 327.3)	Diazepam (285.1 → 257.1)	A, B, D
Repaglinide (453.3 → 230.2)	Diazepam (285.1 → 257.1)	A, B, D
Repaglinide glucuronide (629.4 → 230.4)	Diazepam (285.1 → 257.1)	A, B, D
Rosuvastatin (482.3 → 258.2)	Diazepam (285.1 → 257.1)	A, B, D
Telmisartan (515.1 → 276.1)	Diazepam (285.1 → 257.1)	A, B, D
Telmisartan glucuronide (691.5 → 515.4)	Diazepam (285.1 → 257.1)	A, B, D
Valsartan (436.5 → 235.5)	Diazepam (285.1 → 257.1)	A, B, D

A Waters Alliance 2795 connected with Waters Quattro Ultima triple quadruple mass spectrometer (Waters, Milford, MA) was used for LC MS/MS analyses. A Luna Phenyl Hexyl column 3 µm, 50 × 46 mm (Phenomenex, Torrance, CA) was used as an analytical column for drugs except for pitavastatin (Luna C18 column 3 µm, 50 × 46 mm).

A, 0.05% formic acid in water/methanol mixture (9:1, v/v); B, 0.05% formic acid in water/methanol (1:9, v/v); C, 1 mM ammonium acetate in water/methanol (9:1, v/v); D, 1 mM ammonium acetate in water/methanol (1:9, v/v)

Table S2: LC-MS/MS conditions for protein binding and in vivo studies

Analyte (<i>m/z</i>)	Internal Standard (<i>m/z</i>)	Mobile Phase
Atorvastatin (559.3 → 440.4)	Atorvastatin D5 (564.3 → 445.4)	A, B
Cerivastatin (461.3 → 356.3)	Eli Lilly Proprietary Compound	A, B
Fexofenadine (502.3 → 171.2)	Fexofenadine D6 (508.3 → 177.2)	A, C
Pitavastatin (422.3 → 290.3)	Eli Lilly Proprietary Compound	A, B
Pravastatin (423.2 → 321.0)	Pravastatin D3 (426.2 → 321.0)	A, B
Repaglinide (453.3 → 230.1)	Repaglinide D5 (458.3 → 230.1)	A, B
Rosuvastatin (482.2 → 258.2)	Rosuvastatin D6 (488.2 → 264.2)	C, D
Telmisartan (515.3 → 276.2)	Eli Lilly Proprietary Compound	A, E
Valsartan (436.2 → 207.1)	Valsartan D3 (439.2 → 208.1)	C, D

In vivo study samples were analyzed using a Sciex API 6500+ triple quadrupole mass spectrometer (Applied Biosystems/MDS; Foster City, CA) equipped with a TurbolonSpray interface. The pumps were Shimadzu LC-10AD units with a SCL-10A controller (Kyoto, Japan), and a CTC PAL liquid handler (Zwingen Switzerland) was used as the autosampler. Atorvastatin, fexofenadine, pravastatin, repaglinide, telmisartan and valsartan were analyzed using a Kinetex XB C18 2 x 30 column. Cerivastatin and pitavastatin were reanalyzed using an Ace UltraCore SuperC18 2.1 x 30 column and rosuvastatin analyzed using an Betasil javelin C18 2.1 x 20 column.

A, 2M ammonium bicarbonate/ water (25:1000 v/v); B, 2M ammonium bicarbonate/methanol (25:1000 v/v); C, acetonitrile; D, formic acid/ water (10:1000 v/v); E, methanol

Table S3: Data sources for physiological parameters in dogs

Parameters		References		Median
Hepatocellularity	240 ^a	135 ^b	215 ^c	120 ^d 175
(10 ⁶ cells/g liver)				
Liver weight	29.1 ^e	32.9 ^f	32 ^g	32 ^d 32
(g liver/kg)				
Hepatic blood flow	41.0 ^e	41.5 ^f	30.9 ^g	33 ^d 40
(mL/min/kg)				

^aBayliss et al. (1999)^bSzákacs et al. (2001)^cSohlenius-Sternbeck (2006)^dPeters (2012)^eBoxenbaum (1980)^dBrown et al. (1997)^fDavies and Morris (1993)

Table S4: In vivo and in vitro clearance data in rats

	In vivo CL _{total} (mL/min/kg)	In vivo CL _R (mL/min/kg)	In vivo CL _H (mL/min/kg)	f _{UP}	R _B	Observed CL _{int,H} (mL/min/kg)	In vitro CL _{uptake} (μL/min/10 ⁶ cells)	Predicted CL _{int,H} (mL/min/kg)	Fold error
Cerivastatin	17.00 ^a	-	17.00	0.026 ^a	0.70 ^a	938.9	265 ^b	1273	0.74
Fexofenadine	52.80 ^d	8.20 ^d	44.60	0.338 ^d	0.895 ^d	349.9	10.07 ^e	48	7.24
Pitavastatin	18.20 ^f	-	18.20 ^f	0.014 ^f	0.65 ^f	2000.0	207 ^g	994	2.01
Pravastatin	43.70 ^h)	-	43.70 ^h)	0.672 ^h)	0.65 ^h)	407.4	26 ^g	123	3.30
Repaglinide	5.28 ⁱ	-	5.28 ⁱ	0.015 ^j	0.62 ^j	393.9	107 ^g	512	0.77
Rosuvastatin	28.00 ^h)	0.032 ^k	27.97	0.039 ^h)	0.60 ^h)	1718.4	169 ^g	813	2.11
Telmisartan	6.75 ⁱ	-	6.75	0.006 ⁱ	1.00 ⁱ	1228.7	240 ^g	1154	1.06
Valsartan	4.20 ^h)	-	4.20	0.004 ^h)	0.66 ^h)	1140.7	53 ^g	255	4.47
Bosentan	23.00 ^m)	-	23.00	0.011 ⁿ)	0.55 ^p)	4381.0	138 ^g	661	6.63

CL_H was determined from CL_{total} and CL_R. Observed CL_{int,H} was calculated by the well-stirred model shown in eq. 9 with rat hepatic blood flow 80 mL/min/kg^d. The in vitro CL_{uptake} was scaled by a hepatocellularity value of 120 × 10⁶ cells/g liver and rat liver weight of 40 g liver/body weight^q.

^aPaine et al. (2008)

^bIn house data (265 ± 91 μL/min/10⁶ cells, n=3 separate experiments) measured after 2 h culture, followed by uptake studies performed at 1 μM over 2 min as previously^c)

^cDe Bruyn et al. (2018)

^dPoirier et al. (2008)

^eEstimated over 0.1-100 μM range using the conventional 2-step method as reported by Cantrill and Houston (2017)

^fWatanabe et al. (2010)

^gIn vitro CL_{uptake} values were from Ménochet et al. (2012a): parameters were estimated over 0.1-300 μM range using the mechanistic 2-compartment model and corrected for the loss of cells during experiment

^hFukuda et al. (2008)

ⁱLi and Jiang (2012)

^jXiao et al. (2015)

^kNezasa et al. (2002)

^lGardiner and Paine (2011)

^mTreibert et al. (2004)

ⁿCalculated from $R_B = f_{u_p}/f_{u_b}$ with $f_{u_b} = 0.02^\circ$

^oLave et al. (1997)

^pHaematocrit

^qPeters (2012)

Table S5: Individual uptake parameters obtained in the three lots of plated dog hepatocytes

Drugs	Parameters	XVD	XZG	YHF
Atorvastatin	CL _{total} ($\mu\text{L}/\text{min}/10^6\text{cells}$)	140	90.7	91.5
	CL _{passive} ($\mu\text{L}/\text{min}/10^6\text{cells}$)	13.5	11.1	13.9
	CL _{active} ($\mu\text{L}/\text{min}/10^6\text{cells}$)	127	79.5	77.7
Cerivastatin	CL _{total} ($\mu\text{L}/\text{min}/10^6\text{cells}$)	203	137	90.1
	CL _{passive} ($\mu\text{L}/\text{min}/10^6\text{cells}$)	72.2	32.7	29.8
	CL _{active} ($\mu\text{L}/\text{min}/10^6\text{cells}$)	131	104	60.3
Fexofenadine	CL _{total} ($\mu\text{L}/\text{min}/10^6\text{cells}$)	14.8	9.62	3.88
	CL _{passive} ($\mu\text{L}/\text{min}/10^6\text{cells}$)	0.843	4.98	1.40
	CL _{active} ($\mu\text{L}/\text{min}/10^6\text{cells}$)	14.0	4.65	2.47
Pitavastatin	CL _{total} ($\mu\text{L}/\text{min}/10^6\text{cells}$)	146	128	62.0
	CL _{passive} ($\mu\text{L}/\text{min}/10^6\text{cells}$)	38.0	24.8	25.6
	CL _{active} ($\mu\text{L}/\text{min}/10^6\text{cells}$)	108	103	36.4
Pravastatin	CL _{total} ($\mu\text{L}/\text{min}/10^6\text{cells}$)	13.5	8.41	7.44
	CL _{passive} ($\mu\text{L}/\text{min}/10^6\text{cells}$)	1.11	2.12	0.596
	CL _{active} ($\mu\text{L}/\text{min}/10^6\text{cells}$)	12.4	6.29	6.85
Repaglinide	CL _{total} ($\mu\text{L}/\text{min}/10^6\text{cells}$)	185	118	103
	CL _{passive} ($\mu\text{L}/\text{min}/10^6\text{cells}$)	47.6	27.8	35.7
	CL _{active} ($\mu\text{L}/\text{min}/10^6\text{cells}$)	137	89.8	67.3
Rosuvastatin	CL _{total} ($\mu\text{L}/\text{min}/10^6\text{cells}$)	22.9	23.1	25.9
	CL _{passive} ($\mu\text{L}/\text{min}/10^6\text{cells}$)	2.48	1.75	1.49
	CL _{active} ($\mu\text{L}/\text{min}/10^6\text{cells}$)	20.4	21.3	24.4
Telmisartan	CL _{total} ($\mu\text{L}/\text{min}/10^6\text{cells}$)	169	130	104
	CL _{passive} ($\mu\text{L}/\text{min}/10^6\text{cells}$)	43.1	25.8	29.3
	CL _{active} ($\mu\text{L}/\text{min}/10^6\text{cells}$)	126	104	75.1
Valsartan	CL _{total} ($\mu\text{L}/\text{min}/10^6\text{cells}$)	27.3	29.7	34.0
	CL _{passive} ($\mu\text{L}/\text{min}/10^6\text{cells}$)	2.04	0.742	1.33
	CL _{active} ($\mu\text{L}/\text{min}/10^6\text{cells}$)	25.2	28.9	32.6

Data represent the mean value in triplicate.

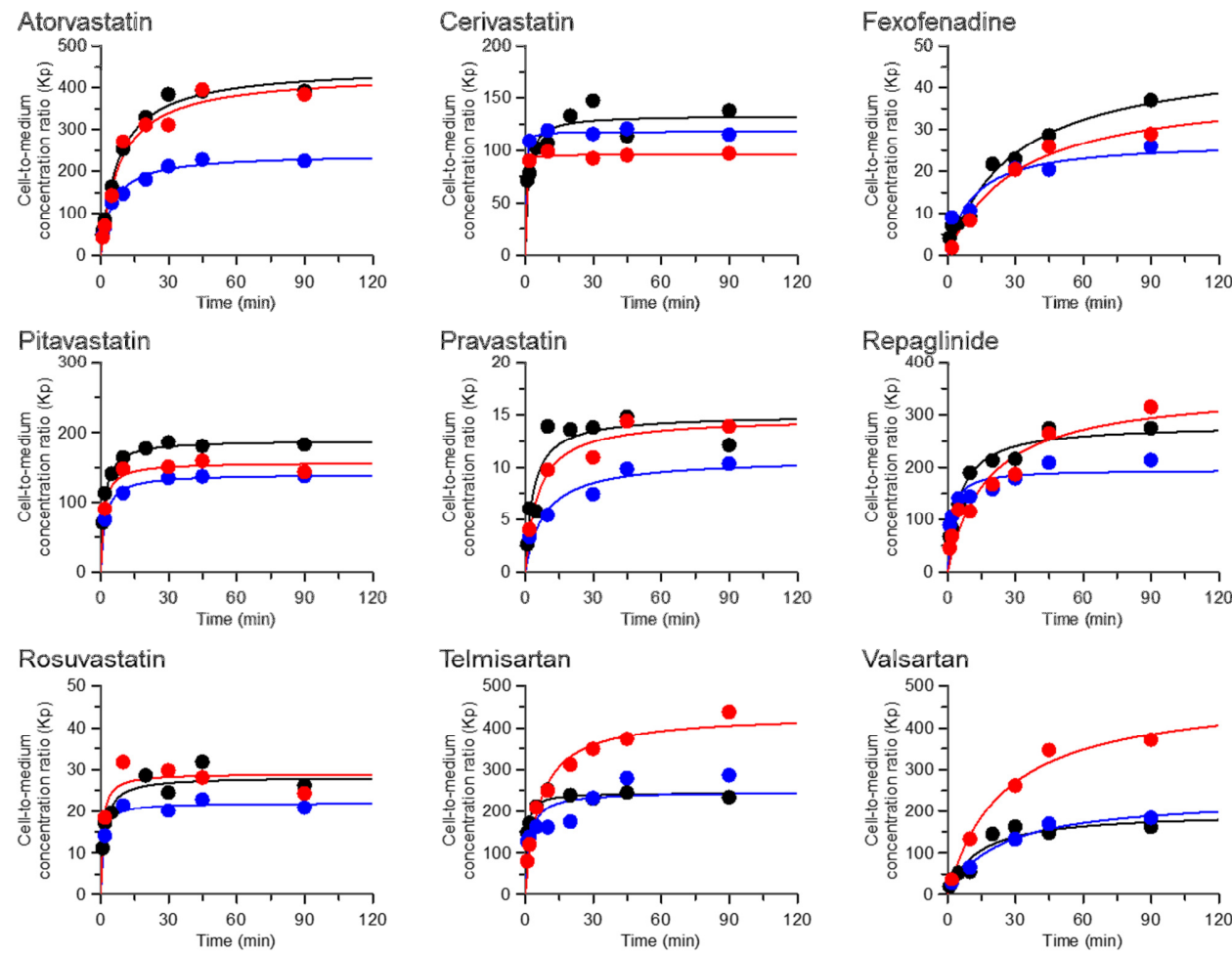


Figure S1: Cell-to-medium concentration ratio (Kp)-time profiles of 9 OATP substrates in three lots of plated dog hepatocytes

Black, blue and red symbols represent the observed data for donors XVD, XZG and YHF, respectively. The solid lines represent the fitting for the corresponding donors. A hyperbolic curve fitting was performed in GraFit v6.0.6 to estimate the maximum Kp at equilibrium.

Table S6: Individual K_p, K_{p_{uu}} and f_{u,cell} parameters obtained in three lots of plated dog hepatocytes

Drugs	Parameters	XVD	XZG	YHF
Atorvastatin	K _p	450	240	434
	K _{p_{uu}}	8.95	6.81	5.96
	f _{u,cell}	0.020	0.028	0.014
Cerivastatin	K _p	133	118	95.7
	K _{p_{uu}}	2.82	4.18	3.02
	f _{u,cell}	0.021	0.035	0.032
Fexofenadine	K _p	48.2	27.1	40.2
	K _{p_{uu}}	17.6	1.93	2.76
	f _{u,cell}	0.365	0.071	0.069
Pitavastatin	K _p	189	140	157
	K _{p_{uu}}	3.84	5.17	2.43
	f _{u,cell}	0.020	0.037	0.015
Pravastatin	K _p	15.0	10.8	14.8
	K _{p_{uu}}	12.2	3.96	12.5
	f _{u,cell}	0.809	0.365	0.845
Repaglinide	K _p	282	195	352
	K _{p_{uu}}	2.69	1.81	1.98
	f _{u,cell}	0.010	0.009	0.006
Rosuvastatin	K _p	28.2	22.0	29.0
	K _{p_{uu}}	9.23	13.2	17.4
	f _{u,cell}	0.327	0.600	0.599
Telmisartan	K _p	244	247	433
	K _{p_{uu}}	1.62	1.39	1.84
	f _{u,cell}	0.007	0.006	0.004
Valsartan	K _p	197	234	489
	K _{p_{uu}}	13.4	40.0	25.5
	f _{u,cell}	0.068	0.171	0.052

Data represent the mean value in duplicate.

Table S7: Comparison of estimated CL_{active} , $CL_{passive}$ and fu_{cell} of rosuvastatin from short and long incubation periods in plated dog hepatocytes (lot XVD)

Drugs	Parameters	Short incubation (from	Long incubation (by
		initial uptake rate and eq. 3)	mechanistic modelling, eq. 4-5)
Cerivastatin	CL_{active} ($\mu L/min/10^6$ cells)	131	201
	$CL_{passive}$ ($\mu L/min/10^6$ cells)	72.2	136
	fu_{cell}	0.021	0.010
Fexofenadine	CL_{active} ($\mu L/min/10^6$ cells)	14	6.93
	$CL_{passive}$ ($\mu L/min/10^6$ cells)	0.843	0.545
	fu_{cell}	0.365	0.391
Pitavastatin	CL_{active} ($\mu L/min/10^6$ cells)	108	149
	$CL_{passive}$ ($\mu L/min/10^6$ cells)	38	70.8
	fu_{cell}	0.024	0.025
Pravastatin	CL_{active} ($\mu L/min/10^6$ cells)	12.4	12.7
	$CL_{passive}$ ($\mu L/min/10^6$ cells)	1.11	2.20
	fu_{cell}	0.809	0.611
Rosuvastatin	CL_{active} ($\mu L/min/10^6$ cells)	20.4	15.3
	$CL_{passive}$ ($\mu L/min/10^6$ cells)	2.48	1.51
	fu_{cell}	0.327	0.293
Valsartan	CL_{active} ($\mu L/min/10^6$ cells)	25.2	34.2
	$CL_{passive}$ ($\mu L/min/10^6$ cells)	2.04	2.73
	fu_{cell}	0.068	0.102

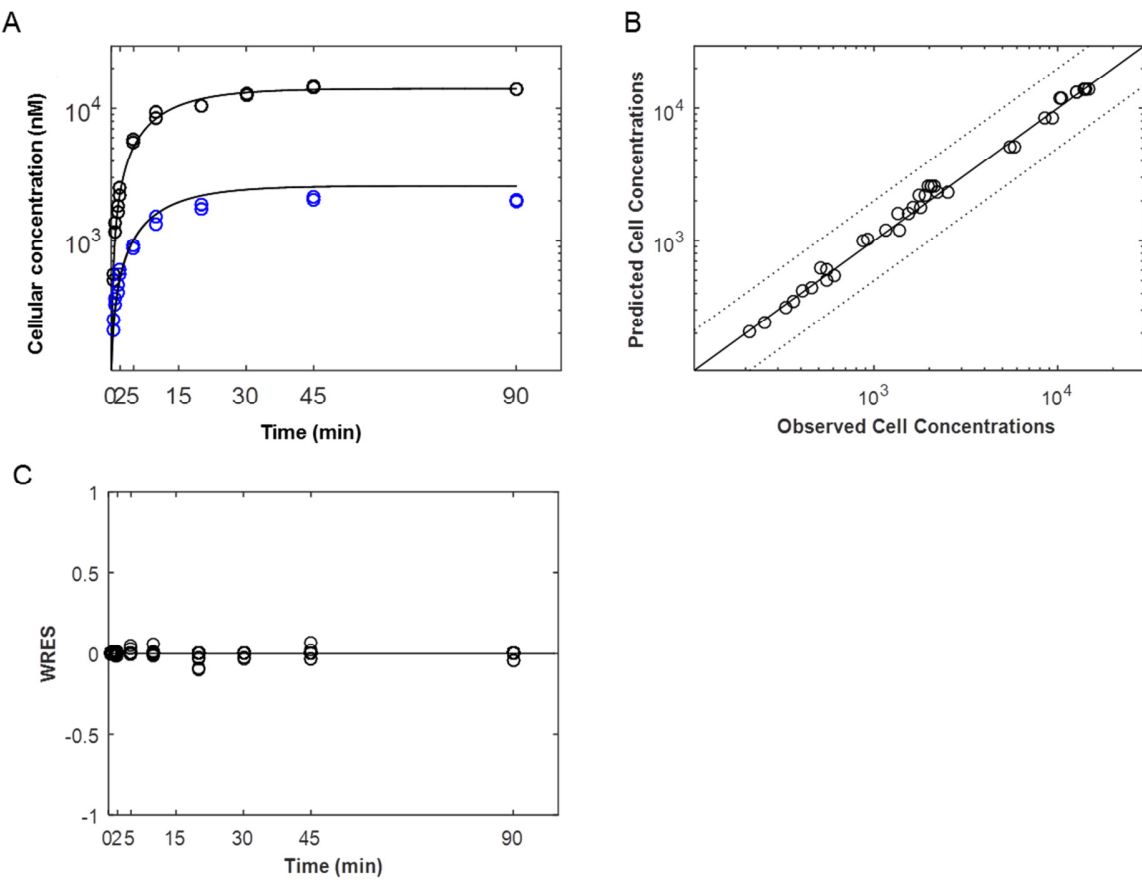


Figure S2: Two compartment mechanistic modelling of rosuvastatin concentration-time profile

Panel A shows cell concentration vs. time profile of rosuvastatin with symbols and black line representing the observed data and model fitting, respectively. Black and blue symbols represent the data in the absence and presence of the cocktail inhibitor. Panel B and C show the goodness of fit and weighted residual error vs. time plots, respectively. The solid and dotted lines in panels B and C represent the line of unity and the 2-fold error, respectively.

Table S8: In vivo and in vitro clearance data in cynomolgus monkeys

	In vivo CL _{total} (mL/min/kg) ^a	In vivo CL _R (mL/min/kg) ^a	In vivo CL _H (mL/min/kg)	f _{up} ^a	R _B ^a	Observed CL _{int,H} (mL/min/kg)	In vitro CL _{uptake} (µL/min/10 ⁶ cells) ^a	Predicted CL _{int,H} (mL/min/kg)	Fold error
Cerivastatin	19.00	-	19.00	0.014	0.76	3181	223	817.0	3.89
Fexofenadine	6.54	1.67 ^a	4.87	0.310	0.55	19	8.00	29.4	0.66
Pitavastatin	10.90	0.11 ^a	10.80	0.026	0.58	723	134	491.7	1.47
Pravastatin	30.00	6.93 ^a	23.10	0.650	0.56	644	9.00	33.0	19.48
Repaglinide	6.89	-	6.89	0.012	0.62	771	129	473.7	1.63
Rosuvastatin	23.70	4.27 ^a)	19.40	0.180	0.69	305	40.1	147.2	2.07
Telmisartan	9.00	-	9.00	0.025	0.78	490	387	1420.7	0.34
Valsartan	6.53	0.62 ^a	5.91	0.014	0.55	560	105	384.8	1.46
Bosentan	17.90	-	17.90	0.061	0.66	776	77.0	281.3	2.76

CL_H was determined from CL_{total} and CL_R. Observed CL_{int,H} was calculated by the well-stirred model shown in eq. 9 with monkey hepatic blood flow 43.6 mL/min/kg^b. The in vitro CL_{uptake} was scaled by a hepatocellularity value of 120 × 10⁶ cells/g liver and monkey liver weight of 30 g liver/body weight^b. R_B values were assumed to be the same as those in humans.

^aDe Bruyn et al. (2018)

^bDavies and Morris (1993)

Table S9: In vivo and in vitro clearance data in humans

	In vivo CL _{total} (mL/min/kg) ^a	In vivo CL _R (mL/min/kg) ^a	In vivo CL _H (mL/min/kg) ^a	f _{UP} ^a	R _B ^a	Observed CL _{int,H} (mL/min/kg) ^a	In vitro CL _{uptake} (μL/min/10 ⁶ cells) ^b	Predicted CL _{int,H} (mL/min/kg)	Fold error
Cerivastatin	2.90	-	2.90	0.002	0.76	1778	244.0	639.1	2.78
Fexofenadine	3.10	1.2	1.9	0.18	0.55	13	8.4	22.0	0.58
Pitavastatin	5.7	-	5.7	0.025	0.58	434	175.6 ± 33.4	459.9 ± 87.6	0.94
Pravastatin	14	6.6	7.4	0.43	0.56	48	6.0	15.8	3.04
Repaglinide	7.8	-	7.8	0.015	0.62	1326	195.2 ± 98.1	511.4 ± 256.9	2.59
Rosuvastatin	10.5	2.9	7.6	0.094	0.69	172	21.3 ± 17.3	55.8 ± 45.3	3.08
Telmisartan	12	-	12	0.005	0.78	9657	370.3 ± 24.4	970.1 ± 63.8	9.96
Valsartan	0.49	0.14	0.35	0.001	0.55	361	8.7 ± 5.8	22.8 ± 15.2	15.8
Bosentan	2.10	-	2.10	0.0053	0.66	468	95.2 ± 18.7	249.3 ± 49.0	1.88

CL_H was determined from CL_{total} and CL_R. Observed CL_{int,H} was calculated by the well-stirred model shown in eq. 9 with human hepatic blood flow 20.7 mL/min/kg^d.

The in vitro CL_{uptake} was scaled by a hepatocellularity value of 120 × 10⁶ cells/g liver and human liver weight of 21.4 g liver/body weight^e.

^aDe Bruyn et al. (2018)

^bData represent mean ± SD of n=4 donors reported in De Bruyn et al. (2018) and Ménochet et al. (2012b)^c, except for pravastatin (n=2), cerivastatin (n=1) and fexofenadine (n=1). The same applies for CL_{active} whereas for CL_{passive}, represent mean of n=2 donors except for cerivastatin and fexofenadine (n=1), and rosuvastatin and repaglinide (n=4) (Ménochet et al., 2012b; De Bruyn et al., 2018)

^cData from Ménochet et al. (2012b) were corrected for cell loss during uptake experiment

^dDavies and Morris (1993)

^eRawden et al. (2005)

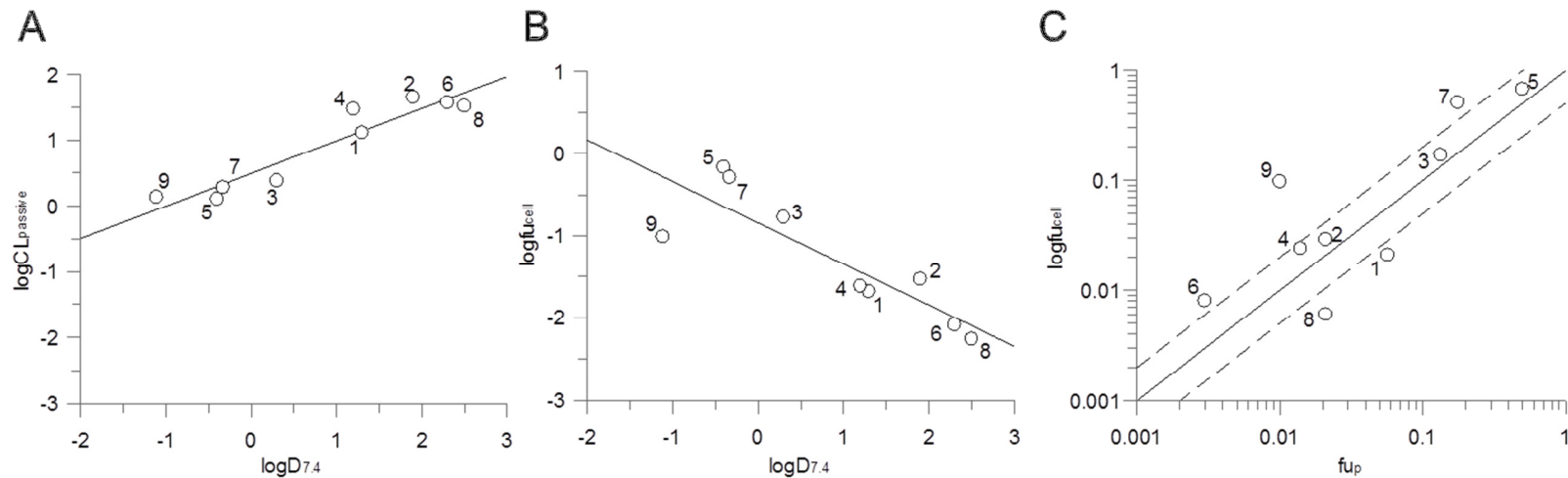


Figure S3: Correlation of CL_{passive} and fu_{cell} values with physicochemical properties logD_{7.4} and relationship between fu_{cell} and fu_p

The log-transformed CL_{passive} (A) and fu_{cell} (B) values of 9 drugs investigated were compared with their physicochemical properties, logD_{7.4}. Correlation between the observed fu_{cell} and fu_p (C) of 9 drugs was investigated. (A) Relationship between parameters was described by the following equation: $\log\text{CL}_{\text{passive}} = 0.492 \times \log\text{D}_{7.4} + 0.494$ ($r^2 = 0.893$). (B) The solid and dashed lines represent the line of unity and 2-fold difference, respectively. (C) Relationship between parameters was described by the following equation: $\log\text{fu}_{\text{cell}} = -0.502 \times \log\text{D}_{7.4} - 0.843$ ($r^2 = 0.751$). 1, atorvastatin; 2, cerivastatin; 3, fexofenadine; 4, pitavastatin; 5, pravastatin; 6, repaglinide; 7, rosuvastatin; 8, telmisartan; 9, valsartan

References

- Bayliss MK, Bell JA, Jenner WN, Park GR, and Wilson K (1999) Utility of hepatocytes to model species differences in the metabolism of loxidine and to predict pharmacokinetic parameters in rat, dog and man. *Xenobiotica* **29**:253-268.
- Boxenbaum H (1980) Interspecies variation in liver weight, hepatic blood flow, and antipyrine intrinsic clearance: extrapolation of data to benzodiazepines and phenytoin. *J Pharmacokinet Biopharm* **8**:165-176.
- Brown RP, Delp MD, Lindstedt SL, Rhomberg LR, and Beliles RP (1997) Physiological parameter values for physiologically based pharmacokinetic models. *Toxicol Ind Health* **13**:407-484.
- Cantrill C and Houston JB (2017) Understanding the Interplay Between Uptake and Efflux Transporters Within In Vitro Systems in Defining Hepatocellular Drug Concentrations. *J Pharm Sci* **106**:2815-2825.
- Davies B and Morris T (1993) Physiological parameters in laboratory animals and humans. *Pharm Res* **10**:1093-1095.
- De Bruyn T, Ufuk A, Cantrill C, Kosa RE, Bi YA, Niosi M, Modi S, Rodrigues AD, Tremaine LM, Varma MVS, Galetin A, and Houston JB (2018) Predicting Human Clearance of Organic Anion Transporting Polypeptide Substrates Using Cynomolgus Monkey: In Vitro-In Vivo Scaling of Hepatic Uptake Clearance. *Drug Metab Dispos* **46**:989-1000.
- Fukuda H, Ohashi R, Tsuda-Tsukimoto M, and Tamai I (2008) Effect of plasma protein binding on in vitro-in vivo correlation of biliary excretion of drugs evaluated by sandwich-cultured rat hepatocytes. *Drug Metab Dispos* **36**:1275-1282.
- Gardiner P and Paine SW (2011) The impact of hepatic uptake on the pharmacokinetics of organic anions. *Drug Metab Dispos* **39**:1930-1938.
- Lave T, Dupin S, Schmitt C, Chou RC, Jaeck D, and Coassolo P (1997) Integration of in vitro data into allometric scaling to predict hepatic metabolic clearance in man: application to 10 extensively metabolized drugs. *J Pharm Sci* **86**:584-590.
- Li C and Jiang Y (2012) Analysis of repaglinide enantiomers in pharmaceutical formulations by capillary electrophoresis using 2,6-di-o-methyl-beta-cyclodextrin as a chiral selector. *J Chromatogr Sci* **50**:739-743.
- Ménochet K, Kenworthy KE, Houston JB, and Galetin A (2012a) Simultaneous assessment of uptake and metabolism in rat hepatocytes: a comprehensive mechanistic model. *J Pharmacol Exp Ther* **341**:2-15.
- Ménochet K, Kenworthy KE, Houston JB, and Galetin A (2012b) Use of Mechanistic Modelling to Assess Inter-Individual Variability and Inter-species Differences in Active Uptake in Human and Rat Hepatocytes. *Drug Metab Dispos* **40**:1744-1756.
- Nezasa K, Takao A, Kimura K, Takaichi M, Inazawa K, and Koike M (2002) Pharmacokinetics and disposition of rosuvastatin, a new 3-hydroxy-3-methylglutaryl coenzyme A reductase inhibitor, in rat. *Xenobiotica* **32**:715-727.
- Paine SW, Parker AJ, Gardiner P, Webborn PJ, and Riley RJ (2008) Prediction of the pharmacokinetics of atorvastatin, cerivastatin, and indomethacin using kinetic models applied to isolated rat hepatocytes. *Drug Metab Dispos* **36**:1365-1374.
- Peters SA (2012) *Physiologically-Based Pharmacokinetic (PBPK) Modeling and Simulations: Principles, Methods, and Applications in the Pharmaceutical Industry*. John Wiley & Sons, Inc.
- Poirier A, Lave T, Portmann R, Brun ME, Senner F, Kansy M, Grimm HP, and Funk C (2008) Design, data analysis, and simulation of in vitro drug transport kinetic experiments using a mechanistic in vitro model. *Drug Metab Dispos* **36**:2434-2444.
- Rawden HC, Carlile DJ, Tindall A, Hallifax D, Galetin A, Ito K, and Houston JB (2005) Microsomal prediction of in vivo clearance and associated interindividual variability of six benzodiazepines in humans. *Xenobiotica* **35**:603-625.
- Sohlenius-Sternbeck AK (2006) Determination of the hepatocellularity number for human, dog, rabbit, rat and mouse livers from protein concentration measurements. *Toxicol In Vitro* **20**:1582-1586.
- Szákacs T, Veres Z, and Vereczkey L (2001) In vitro-in vivo correlation of the pharmacokinetics of vincopetine. *Pol J Pharmacol* **53**:623-628.

- Treiber A, Schneiter R, Delahaye S, and Clozel M (2004) Inhibition of organic anion transporting polypeptide-mediated hepatic uptake is the major determinant in the pharmacokinetic interaction between bosentan and cyclosporin A in the rat. *J Pharmacol Exp Ther* **308**:1121-1129.
- Watanabe T, Kusuhara H, Maeda K, Kanamaru H, Saito Y, Hu Z, and Sugiyama Y (2010) Investigation of the rate-determining process in the hepatic elimination of HMG-CoA reductase inhibitors in rats and humans. *Drug Metab Dispos* **38**:215-222.
- Xiao Q, Tang L, Xu R, Qian W, and Yang J (2015) Physiologically based pharmacokinetics model predicts the lack of inhibition by repaglinide on the metabolism of pioglitazone. *Biopharm Drug Dispos* **36**:603-612.